Electronic Supplementary Material (ESI) for Environmental Science: Nano.
This journal is © The Royal Society of Chemistry 2019

Supplementary information for

Template-free synthesis of oxygen-containing ultrathin porous carbon quantum dots/polymeric carbon nitride metal-free composites with superior broad-spectrum photocatalytic activity for PPCPs remediation

Fengliang Wang[1], Yingfei Wang[2], Yuliang Wu[1], Dandan Wei[1], Lei Li[3], Qianxin Zhang[1], Haijin Liu[4], Yang Liu[5], Wenying Lv[1], Guoguang Liu[1*]

[1] *Institute of Environmental Health and Pollution Control, School of Environmental Science and Engineering, Guangdong University of Technology, Guangzhou, 510006, China*

[2] *School of Environmental Science and Engineering, Sun Yat-sen University, Guangzhou 510006, China*

[3] *Key Laboratory of Extraordinary Bond Engineering and Advanced Materials Technology (EBEAM) of Chongqing, Yangtze Normal University, Chongqing 408100, China*

[4] *Key Laboratory for Yellow River and Huaihe River Water Environment and Pollution Control, School of Environment, Henan Normal University, Xinxiang, 453007, China*

[5]*Faculty of Environmental & Biological Engineering, Guangdong University of Petrochemical Technology, Maoming, 525000, China*

* Corresponding Author: Guoguang Liu, E-mail: liugg615@163.com, Phone: +86-20-39322547, Fax: +86-20-39322548

Contents

Text S1. Determination of concentration of IDM 1

Text S2. Intermediates Identification by HRAM LC-MS/MS 1

Text S3. Calculation Details 1

Fig. S1. The model structure of (A) BCN; (B) CQD/BCN, and (C) CQD/OUPCN. 3

Fig. S2. The TEM image (Insert: the HRTEM image) of CQD. 4

Fig. S3. The (A) SEM image and (B) TEM image of BCN. 4

Fig. S4. The TEM images of (A) CQD/BCN-0.5% and (D) CQD/OPUCN-0.5%; The HRTEM images(Insert: FFT) of (D) CQD/BCN-0.5% and (E) CQD/OPUCN-0.5%; The CQD diameter distribution of (C) CQD/BCN-0.5% and (F) CQD/OPUCN-0.5%; 5

Fig. S5. The AFM image of BCN. 5

Fig. S6. (A) XPS spectrum and (B) high-resolution XPS spectrum of N1s of BCN, CQD/BCN-0.5%, and CQD/OUPCN-0.5%. 6

Fig. S7. Nitrogen adsorption–desorption isotherms (Insert: Pore-size distrbution) of CQD/OCN-0.5%. 6

Fig. S8. (A) XPS spectrum and (B) high-resolution XPS spectrum of N1s of BCN, CQD/BCN-0.5%, and CQD/OUPCN-0.5%. 7

Fig. S9. Fragment chart analyses of the HRAM LC-MS ion mass spectrometry of the IDM and its by-products. 10

Fig. S10. Fragment chart analyses of the HRAM LC-MS/MS secondary ion mass spectrometry of the IDM and its by-products. 13

Table S1. Mobile phase composition and gradient elution. 14

Table S2. Mass spectrum parameters. 14

Table S3. Mass spectrum scanning parameters. 14

References 15

TEXT

Text S1. Determination of concentration of IDM

The concentration of IDM was analyzed via Shimadzu LC 20A high performance liquid chromatography (HPLC, Japan) equipped with a C18 reversed-phase column (Zorbax Eclipse, 4.6 × 250 mm, 5 μm). The isocratic elution consisted of 70 % methanol and 30 % water containing 0.2 % (v/v) formic acid, with a flow rate of 1 $mL \cdot min^{-1}$. The detection wavelength was set at 270 nm.

Text S2. Intermediates Identification by HRAM LC-MS/MS

The photocatalytic degradation intermediates of IDM were identified by Thermo Scientific Ultimate 3000 RSLC High Resolution liquid chromatography coupled with Q Exactive Orbitrap mass spectrometry. Separation was accomplished using an Hypersil GOLD C18 (100 x 2.1 mm, 1.9 μm) with column temperature 40 ℃. Elution was performed at a flow rate of 0.3 mL/min with water that contained 0.1 % (v/v) formic acid as eluent A, and methanol as eluent B. Mass spectral analysis was conducted in negative mode. Mass spectral analysis was conducted in negative mode. The mobile phase composition and mass spectrum scanning parameters have been listed in Table S1 to S3.

Text S3. Calculation Details

The electron-electron exchange and correlation interactions were described by using the generalized gradient approximation (GGA) with the form of the Perdew-Burke-

Ernzerhof (PBE)[s1] functional. The projector augmented wave (PAW) [s2, s3] method was employed to describe the interaction between the core and valence electrons. The wave functions were expanded in a plane wave basis sets with a cutoff energy of 500 eV. The convergence criteria for the electronic self-consistent iteration and the ionic relaxation loop were set as the values of 1×10^{-5} eV and 1×10^{-4} eV/Å, respectively. Brillouin zone integrations were performed with k-point sampling using Monkhorst-Pack (MP)[s4] of $5 \times 5 \times 1$ for the models. The method of Gaussian smearing was employed to determine the valence electrons occupancies with a smearing width of 0.05 eV.

The optimized structure of BCN, CQD/BCN, and CQD/OUPCN were dispicted in Fig. S1. The vacuum space was more than 15 Å, which was enough to avoid the interaction between periodical images. The lattice constant of BCN was calculated to be 7.13 Å which agrees to the published results [s5, s6].

FIGURES

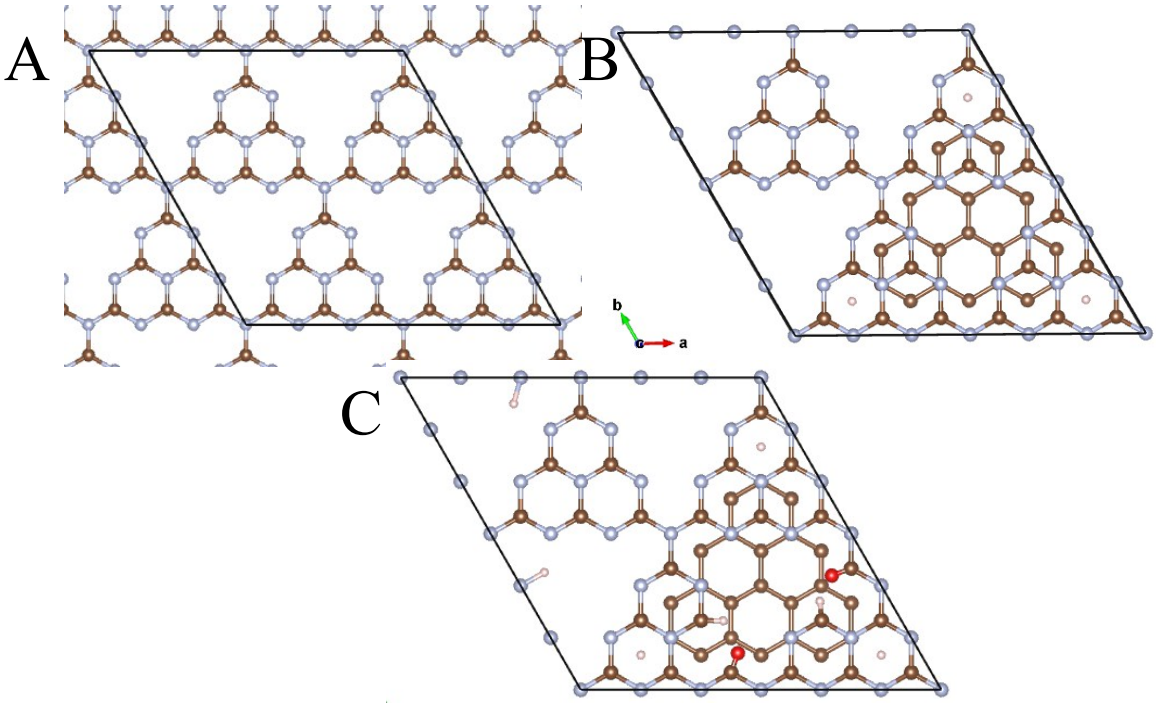

Fig. S1. The model structure of (A) BCN; (B) CQD/BCN, and (C) CQD/OUPCN.

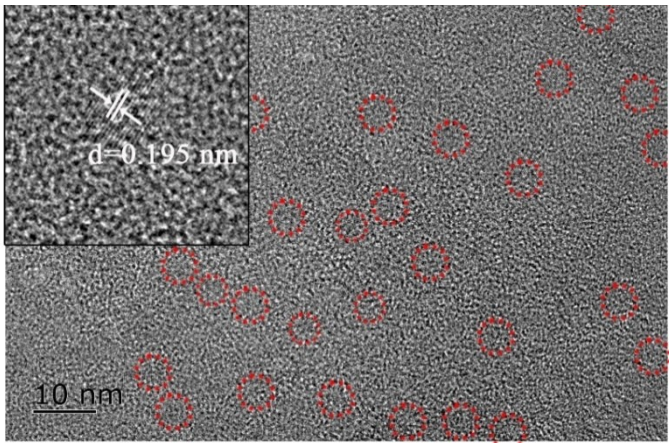

Fig. S2. The TEM image (Insert: the HRTEM image) of CQD.

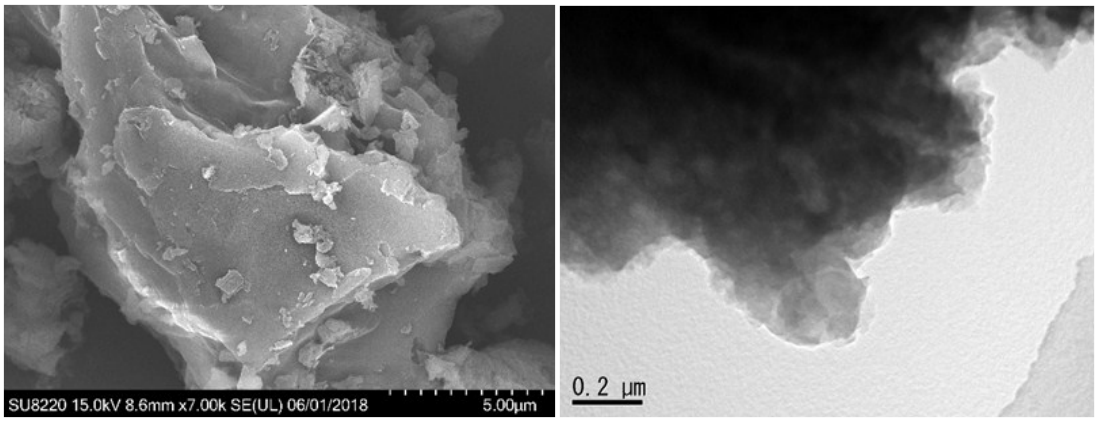

Fig. S3. The (A) SEM image and (B) TEM image of BCN.

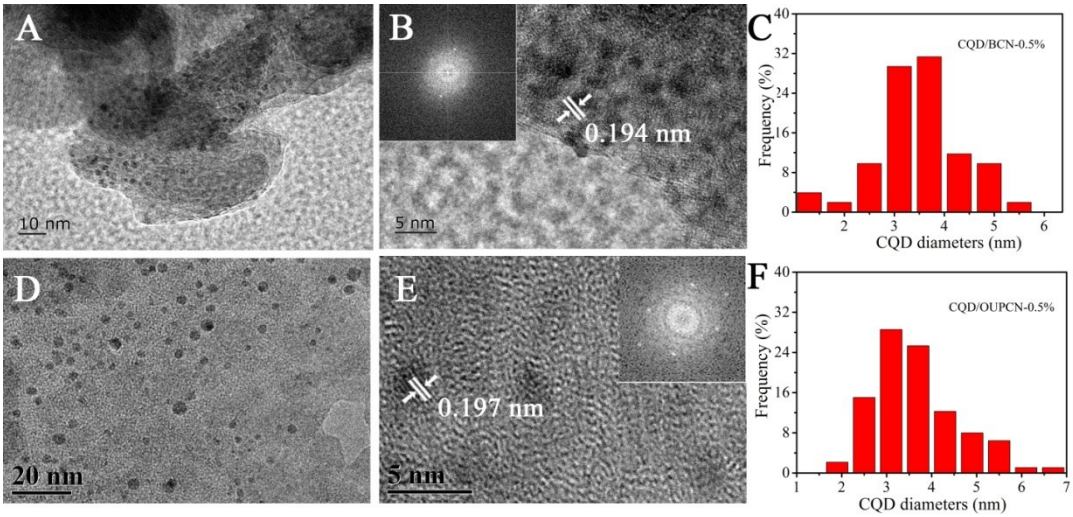

Fig. S4. The TEM images of (A) CQD/BCN-0.5% and (D) CQD/OPUCN-0.5%; The HRTEM images (Insert: Fourier transform pattern) of (D) CQD/BCN-0.5% and (E) CQD/OPUCN-0.5%; The CQD diameter distribution of (C) CQD/BCN-0.5% and (F) CQD/OPUCN-0.5%;

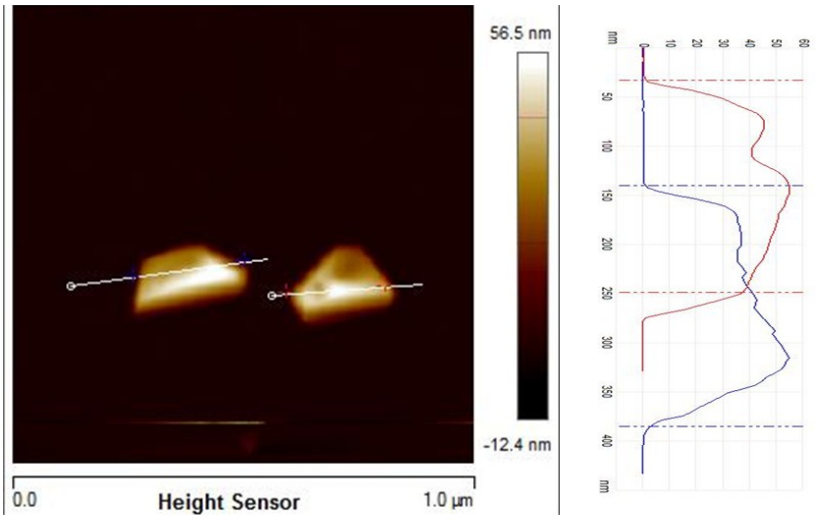

Fig. S5. The AFM image of BCN.

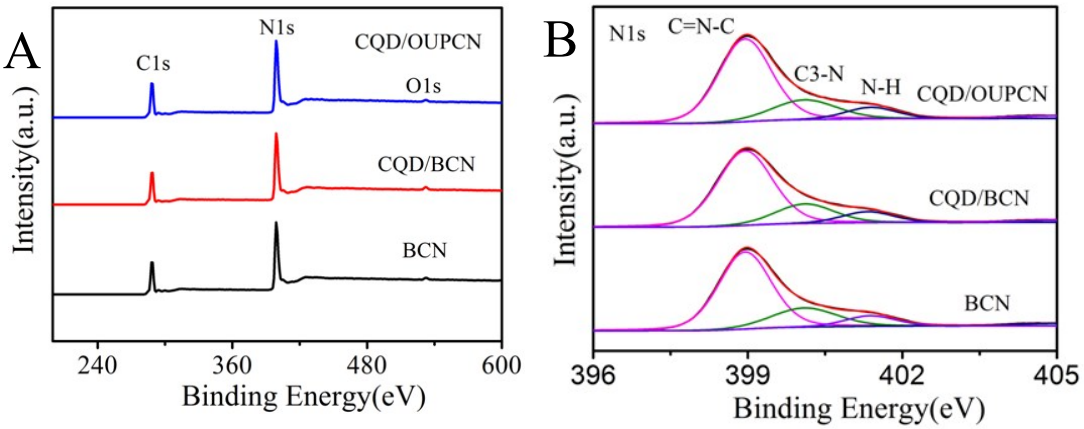

Fig. S6. (A) XPS spectrum and (B) high-resolution XPS spectrum of N1s of BCN, CQD/BCN-0.5%, and CQD/OUPCN-0.5%.

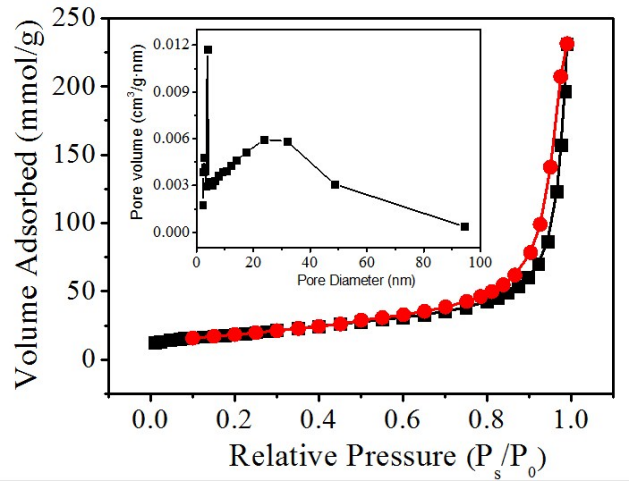

Fig. S7. **Nitrogen adsorption–desorption isotherms (Insert: Pore-size distribution) of CQD/OCN-0.5%.**

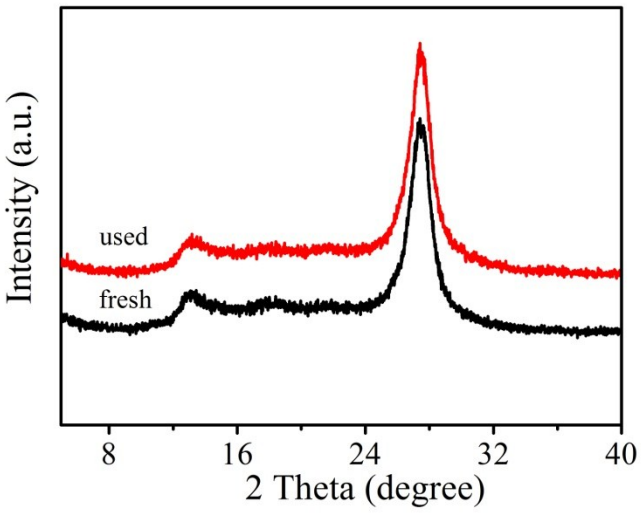

Fig. S8. (A) XPS spectrum and (B) high-resolution XPS spectrum of N1s of BCN, CQD/BCN-0.5%, and CQD/OUPCN-0.5%.

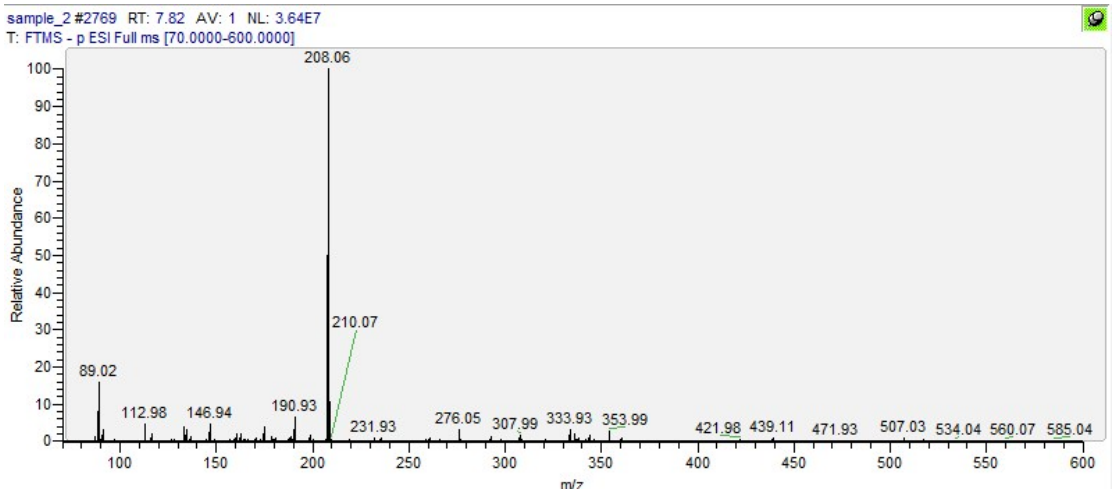
sample_2 #2769 RT: 7.82 AV: 1 NL: 3.64E7
T: FTMS - p ESI Full ms [70.0000-600.0000]
208.06
210.07
89.02
112.98
146.94
190.93
231.93
276.05
307.99
333.93
353.99
421.98
439.11
471.93
507.03
534.04
560.07
585.04
Relative Abundance
m/z

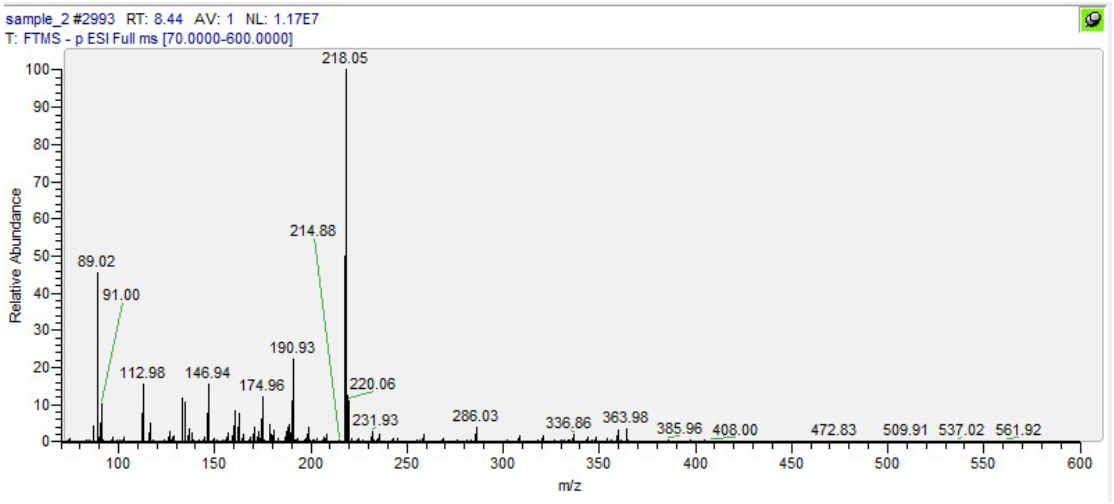
sample_2 #2993 RT: 8.44 AV: 1 NL: 1.17E7
T: FTMS - p ESI Full ms [70.0000-600.0000]
218.05
214.88
89.02
91.00
190.93
112.98
146.94
174.96
220.06
231.93
286.03
336.86
363.98
385.96
408.00
472.83
509.91
537.02
561.92
Relative Abundance
m/z

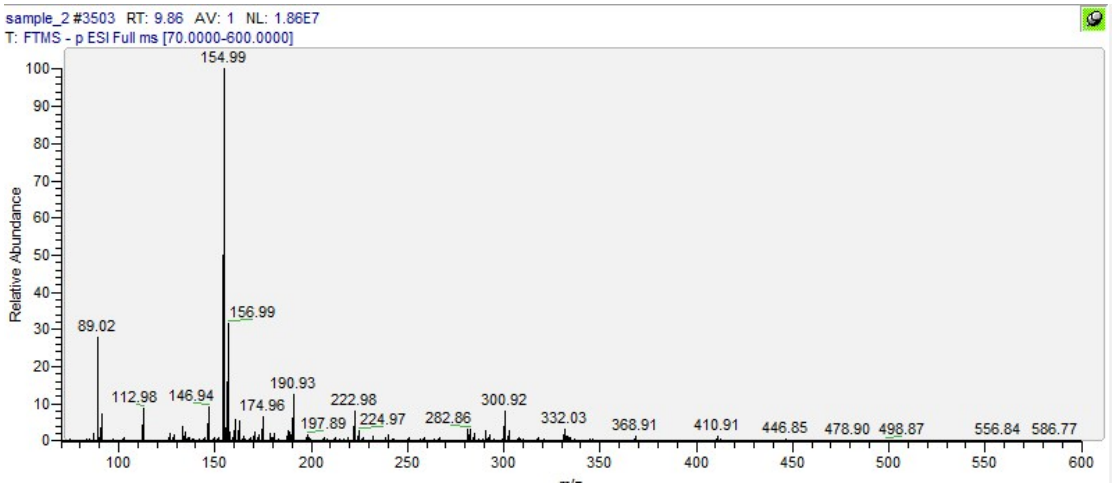
sample_2 #3503 RT: 9.86 AV: 1 NL: 1.86E7
T: FTMS - p ESI Full ms [70.0000-600.0000]
154.99
156.99
89.02
112.98
146.94
174.96
190.93
197.89
222.98
224.97
282.86
300.92
332.03
368.91
410.91
446.85
478.90
498.87
556.84
586.77
Relative Abundance

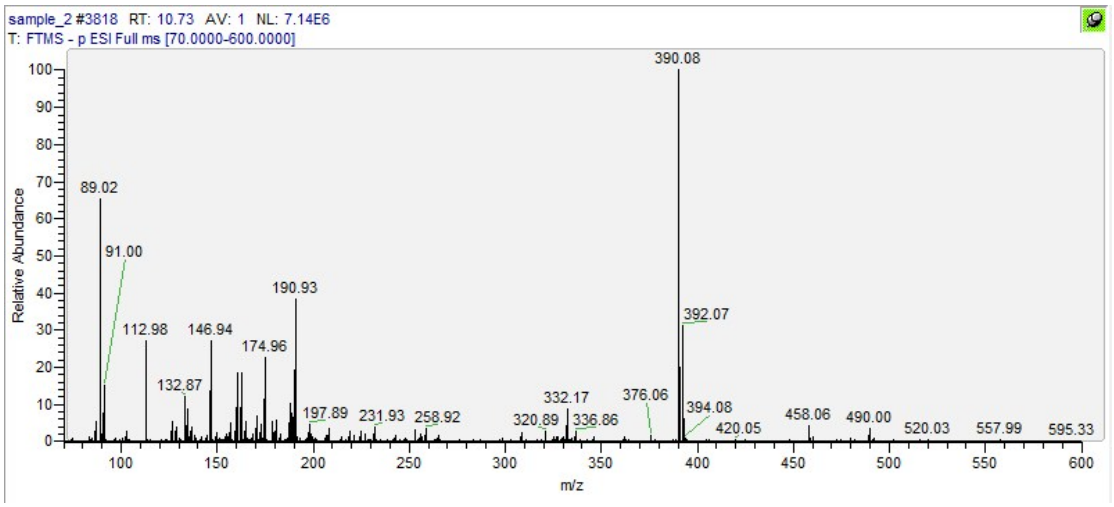
sample_2 #3818 RT: 10.73 AV: 1 NL: 7.14E6
T: FTMS - p ESI Full ms [70.0000-600.0000]
Relative Abundance
m/z
390.08
89.02
91.00
190.93
392.07
112.98
146.94
174.96
132.87
332.17
376.06
197.89
231.93
258.92
320.89
336.86
394.08
420.05
458.06
490.00
520.03
557.99
595.33

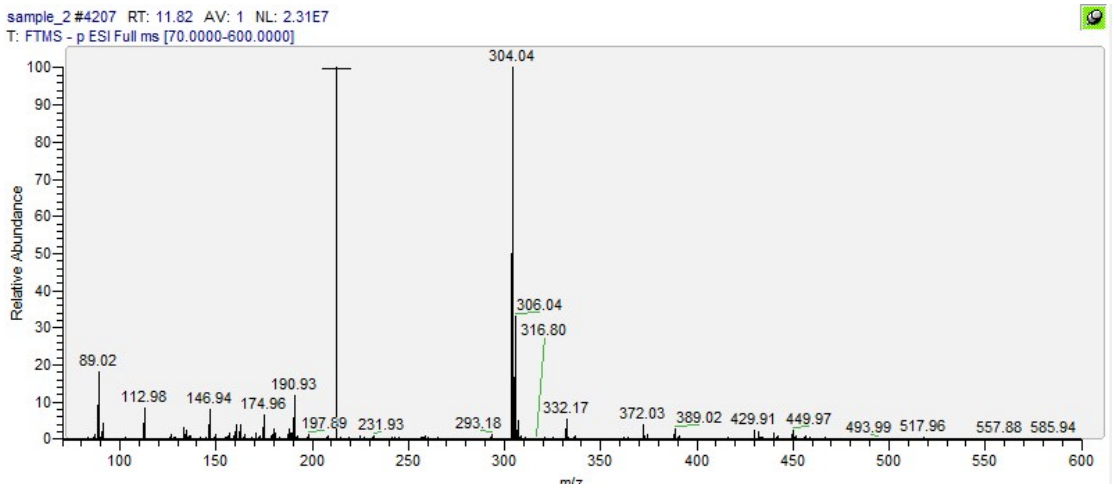
sample_2 #4207 RT: 11.82 AV: 1 NL: 2.31E7
T: FTMS - p ESI Full ms [70.0000-600.0000]
Relative Abundance
m/z
304.04
306.04
316.80
89.02
190.93
112.98
146.94
174.96
197.69
231.93
293.18
332.17
372.03
389.02
429.91
449.97
493.99
517.96
557.88
585.94

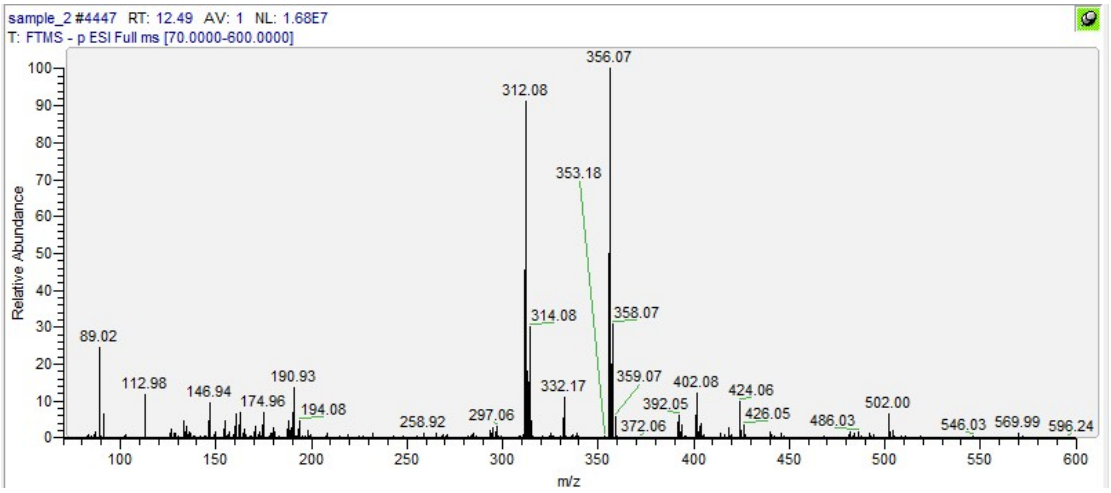
sample_2 #4447 RT: 12.49 AV: 1 NL: 1.68E7
T: FTMS - p ESI Full ms [70.0000-600.0000]
Relative Abundance
m/z
356.07
312.08
353.18
314.08
358.07
89.02
359.07
402.08
424.06
112.98
146.94
190.93
174.96
194.08
332.17
392.05
426.05
502.00
258.92
297.06
372.06
486.03
546.03
569.99
596.24

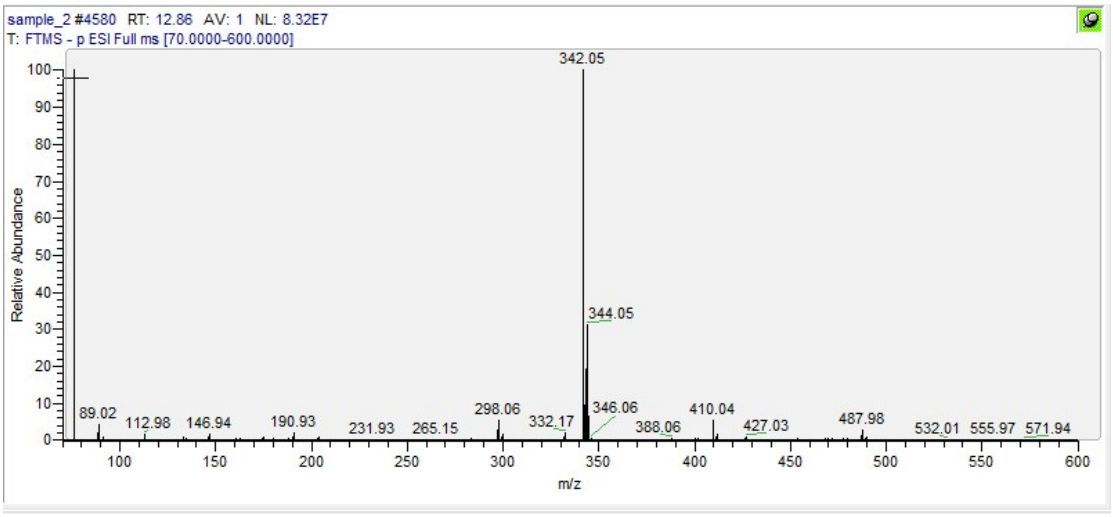

Fig. S9. Fragment chart analyses of the HRAM LC-MS ion mass spectrometry of the IDM and its by-products.

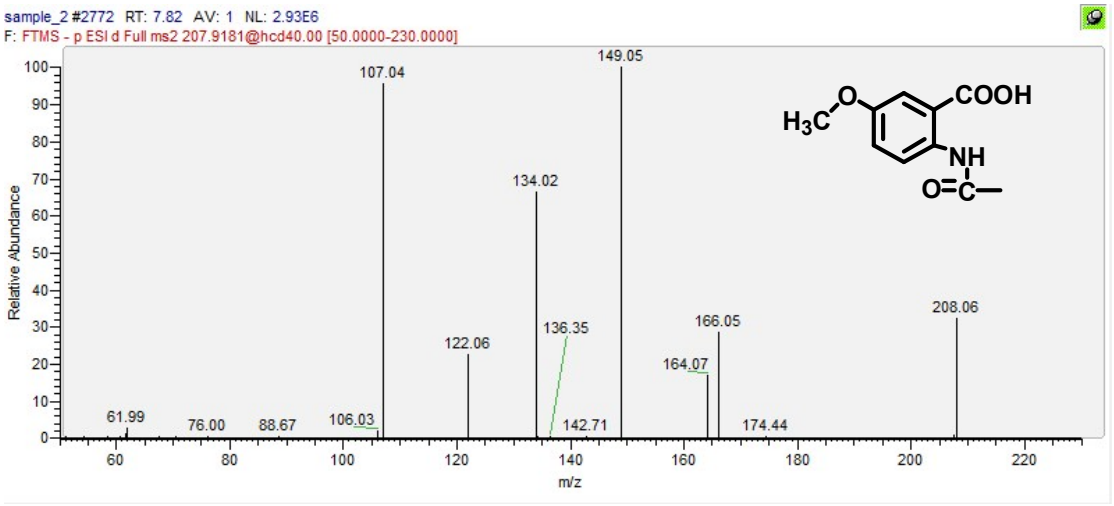
sample_2 #2772 RT: 7.82 AV: 1 NL: 2.93E6
F: FTMS - p ESI d Full ms2 207.9181@hcd40.00 [50.0000-230.0000]
Relative Abundance
m/z
149.05
107.04
134.02
208.06
166.05
122.06
136.35
164.07
61.99
76.00
88.67
106.03
142.71
174.44
COOH
NH
O=C
H3C
O

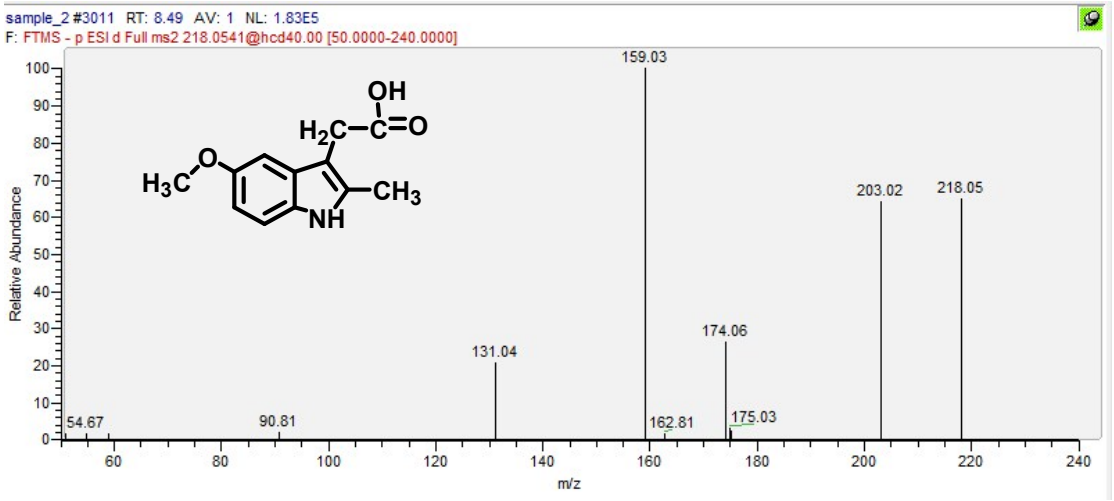
sample_2 #3011 RT: 8.49 AV: 1 NL: 1.83E5
F: FTMS - p ESI d Full ms2 218.0541@hcd40.00 [50.0000-240.0000]
Relative Abundance
m/z
159.03
203.02
218.05
174.06
131.04
54.67
90.81
162.81
175.03
OH
H2C
C=O
H3C
O
CH3
NH

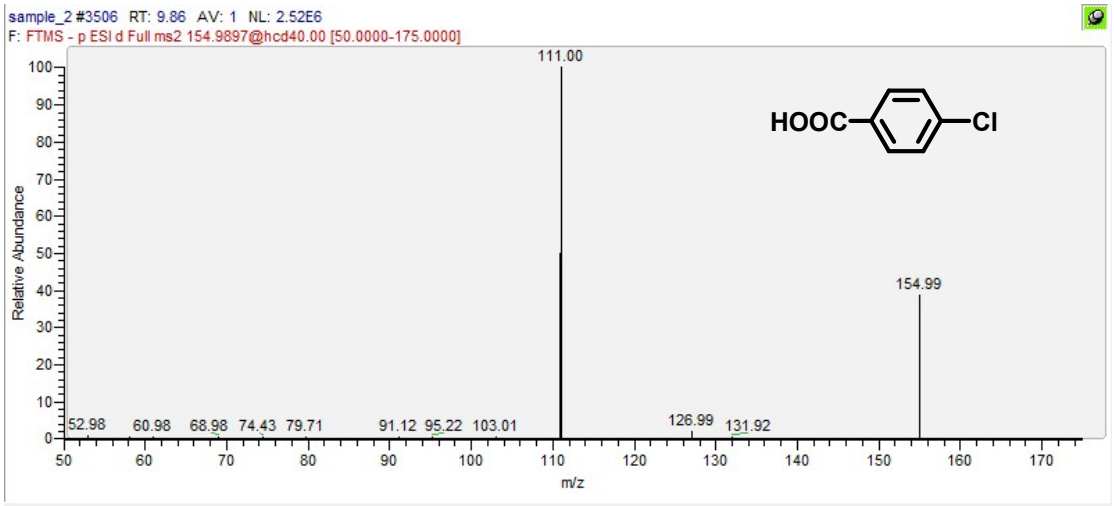
sample_2 #3506 RT: 9.86 AV: 1 NL: 2.52E6
F: FTMS - p ESI d Full ms2 154.9897@hcd40.00 [50.0000-175.0000]
Relative Abundance
m/z
111.00
154.99
52.98
60.98
68.98
74.43
79.71
91.12
95.22
103.01
126.99
131.92
HOOC
Cl

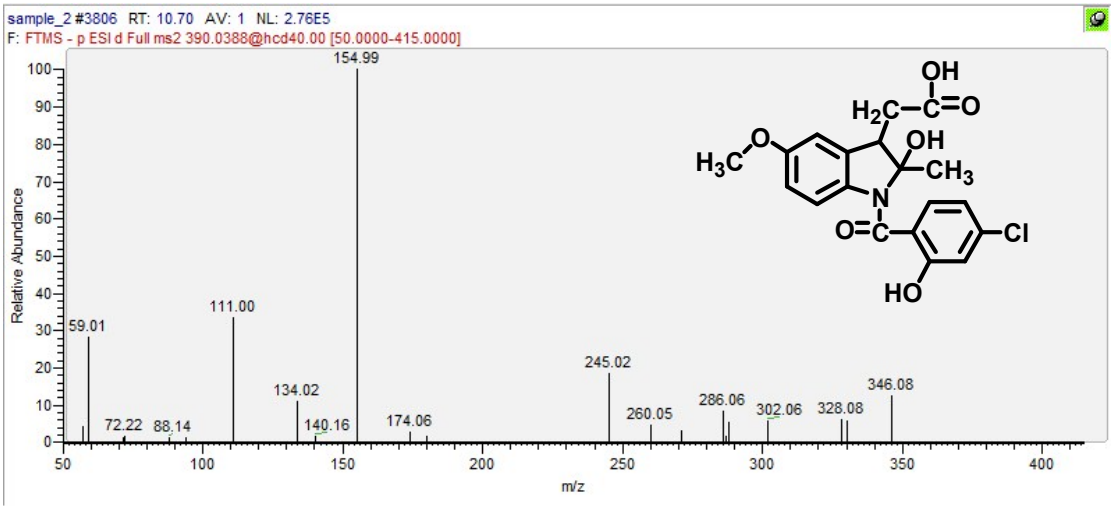
sample_2 #3806 RT: 10.70 AV: 1 NL: 2.76E5
F: FTMS - p ESI d Full ms2 390.0388@hcd40.00 [50.0000-415.0000]
Relative Abundance
m/z
154.99
111.00
59.01
134.02
245.02
346.08
286.06
260.05
302.06
328.08
72.22
88.14
140.16
174.06
OH
H2C
C=O
OH
CH3
H3C
O
N
O=C
Cl
HO

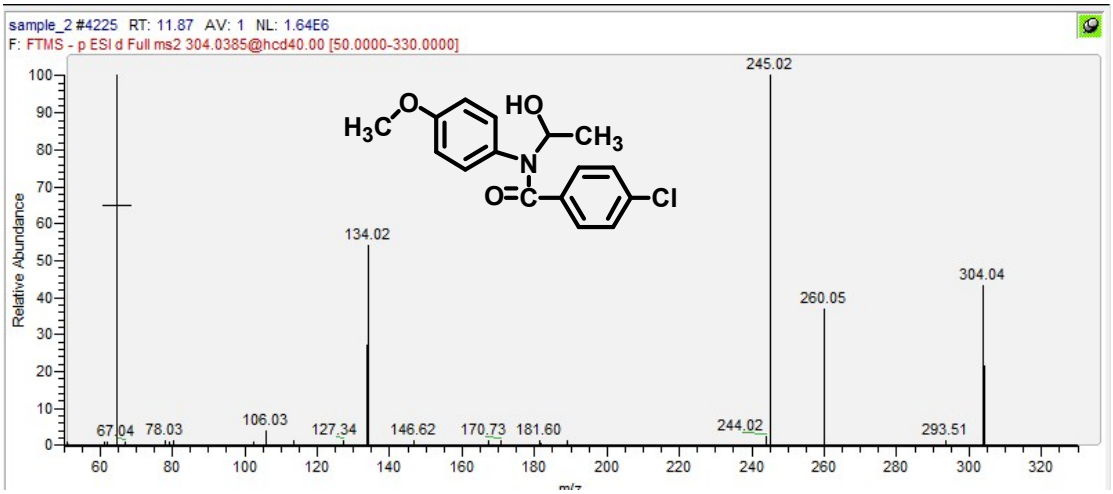
sample_2 #4225 RT: 11.87 AV: 1 NL: 1.64E6
F: FTMS - p ESI d Full ms2 304.0385@hcd40.00 [50.0000-330.0000]
Relative Abundance
245.02
134.02
304.04
260.05
67.04
78.03
106.03
127.34
146.62
170.73
181.60
244.02
293.51
H3C
O
HO
CH3
N
O=C
Cl

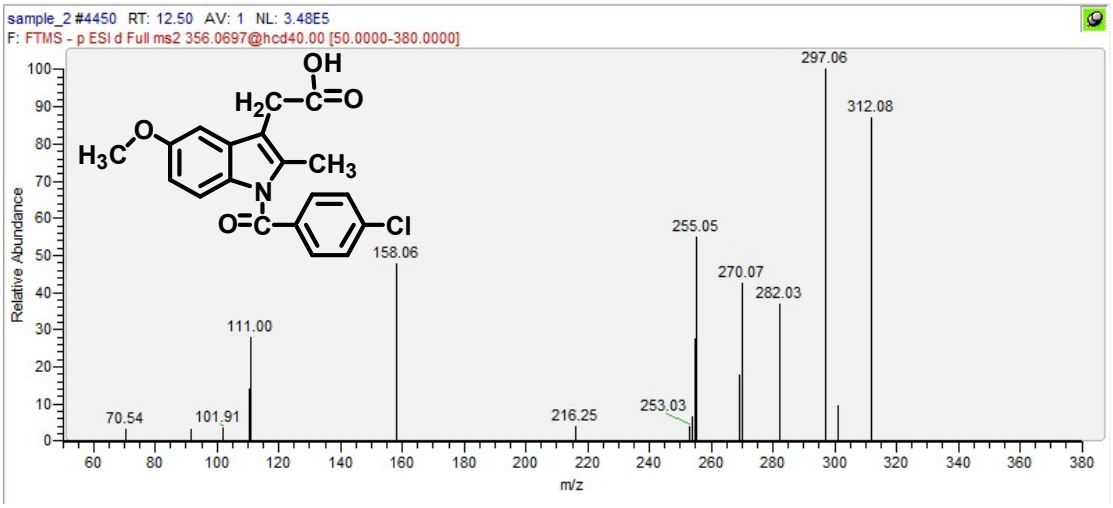
sample_2 #4450 RT: 12.50 AV: 1 NL: 3.48E5
F: FTMS - p ESI d Full ms2 356.0697@hcd40.00 [50.0000-380.0000]
Relative Abundance
m/z
297.06
312.08
255.05
158.06
270.07
282.03
111.00
70.54
101.91
216.25
253.03
OH
H2C
C=O
H3C
O
CH3
N
O=C
Cl

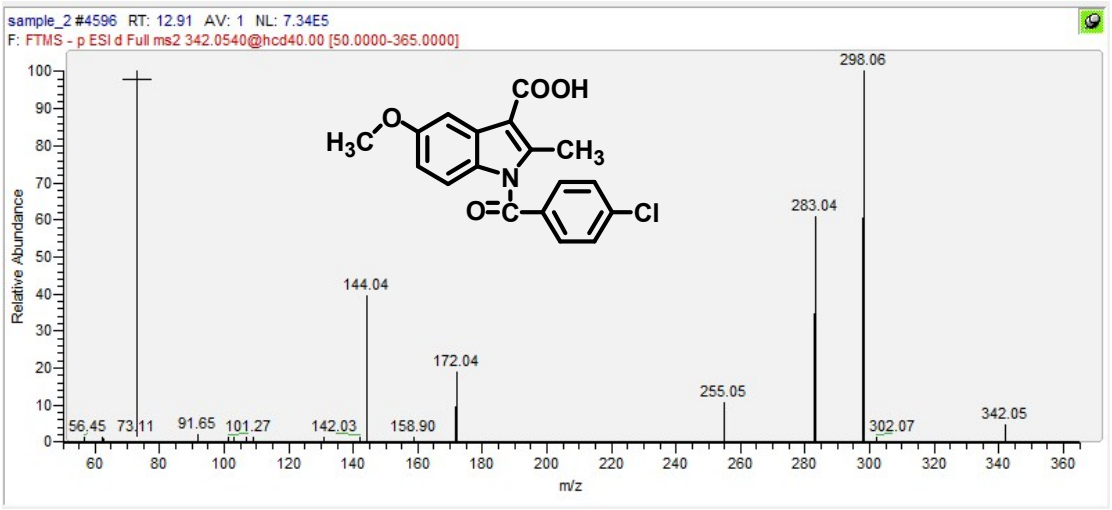

Fig. S10. Fragment chart analyses of the HRAM LC-MS/MS secondary ion mass spectrometry of the IDM and its by-products.

TABLE

Table S1. Mobile phase composition and gradient elution.

Time (min)	%A	%B
0	98	2
2	98	2
16	5	95
18	5	95
18.1	98	2
20	98	2

Table S2. Mass spectrum parameters.

Mass spectrum parameters	Value
Sheath gas flow rate	40
Aux gas flow rate	10
Sweep gas flow rate	0
Spray voltage (lKVl)	+3.5，-2.5
Capillary temp. (℃)	320
Aux gas heater temp. (℃)	350

Table S3. Mass spectrum scanning parameters.

Mass spectrum scanning parameters	Value
Scan mode	Full MS-ddMS2
Full MS scan range	70-600 m/z
Resolution	Full MS: 70,000 FWHM
	MS/MS: 17,500 FWHM
Isolation width	2.0 m/z
NCE (Stepped NCE)	40 (50%)

References

S1. Perdew, J. P., Burke, K. & Ernzerhof, M. Phys. Rev. Lett. 77, 3865–3868 (1996).

S2. Kresse, G. & Joubert, D. Phys. Rev. B 59, 1758–1775 (1999).

S3. Blöchl, P. E. Phys. Rev. B 50, 17953–17979 (1994).

S4. Hendrik J. Monkhorst, J. D. P. Phys. Rev. B 13, 5188–5192 (1976).

S5. Xinguo Ma, Yanhui Lv, Jing Xu, Yanfang Liu, Ruiqin Zhang, and Yongfa Zhu. J. Phys. Chem. C, 116, 23485−23493 (2012).

S6. Bicheng Zhu, Jinfeng Zhang, Chuanjia Jiang, Bei Cheng, Jiaguo Yu. Appl. Catal. B: Env. 207, 27-34 (2017)